# Simulations of bremsstrahlung and synchrotron radiation from runaway electrons

M. Hoppe, O. Embréus, P. Svensson, L. Unnerfelt, T. Fülöp

*Chalmers University of Technology, SE-41295, Göteborg, Sweden*

Highly energetic runaway electrons (RE) primarily emit two types of radiation: bremsstrahlung (BR) and synchrotron (SR). The former is emitted mainly in collisions with the stationary background plasma while the latter results from continuous acceleration experienced by the particle in the tokamak magnetic field. Both types of radiation are routinely used to diagnose runaway electrons at several tokamaks around the world [1, 2] and recent modelling efforts [3, 4, 5] provide more detailed simulations than ever before.

In this paper we present recent developments of the synthetic diagnostic *Synchrotron-detecting Orbit Following Toolkit* (SOFT) [6] which extends the code to permit studies of RE bremsstrahlung, as well as the polarization of synchrotron radiation. We also analyze the effect and importance of drift orbits on the detected synchrotron radiation by accounting for the first order corrections in guiding-center theory.

**Bremsstrahlung** The mechanisms through which BR and SR are generated are very different, and as a result the distribution of radiation within the observed spot depends on energy and pitch-angle in completely different ways. In particular, as was shown in [5], SR spots tend to appear significantly brighter on the high field side due to the very strong dependence of the emission on pitch angle and magnetic field strength. Since BR is independent of both, bremsstrahlung spots tend to have a more uniform distribution of radiation across the spot (cf. Figs. 1(a) & (b)).

The different energy and pitch angle dependences also influence which electrons in any given RE distribution that dominate emission, or in other words, which parts of momentum

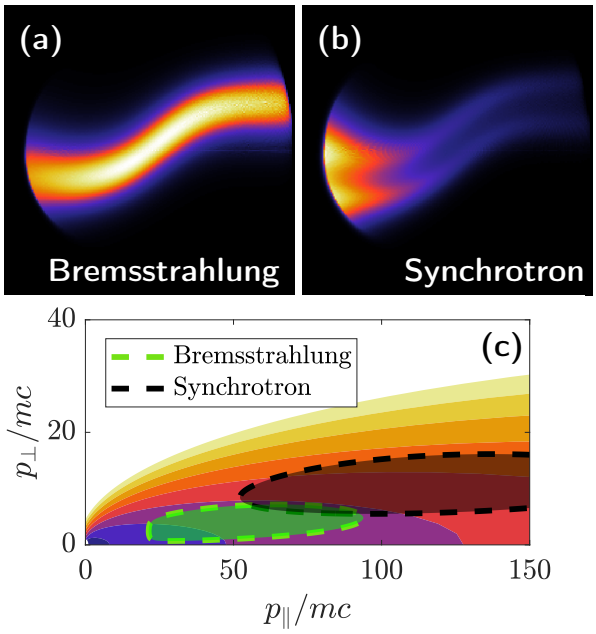


Figure 1: Simulated (a) bremsstrahlung and (b) synchrotron images resulting from the distribution function in (c). Also shown super-imposed in (c) are the regions of dominant BR (green) and SR (black) emission which contribute to the images.

space that can be probed. Figure 1 shows the (a) BR and (b) SR images resulting from the distribution function in (c). Super-imposed over the distribution function in Fig. 1 are the regions of momentum-space dominating BR and SR emission respectively.

**Polarization of synchrotron radiation** The emitted SR consists of two polarization components, one in the orbit plane and one in the perpendicular direction. Using a linear polarization filter the linear polarization of SR in the detector plane can be measured, and its intensity can be expressed in terms of the Stokes parameters $I$, $Q$, $U$ as well as the rotation angle $\psi$ of the polarization filter [7]:

$$I_{\mathrm{lin}}(\psi) = \frac{1}{2}\left(I + Q\cos 2\psi + U\sin 2\psi\right). \tag{1}$$

By placing a quarter-wave plate (and a wavelength filter to only transmit monochromatic light) in front of the linear polarization filter one can also gain information about the circular polarization component which has a similar dependence on $I$, $Q$ and $\psi$ as the linear polarization in Eq. (1), but with $U$ replaced by Stokes $V$ parameter. By measuring with the linear polarizer at three angles (0°, 45° and 90°) and also with the quarter wave plate at 45°, sufficient information is obtained to solve for the four Stokes parameters, which contain all information about the polarization of the SR.

The Stokes parameters $I$, $Q$ and $U$ all depend very similarly on particle Lorentz factor $\gamma$ and pitch angle $\theta_{\mathrm{p}}$, meaning that both linear polarization components result from almost exactly the same part of the RE distribution function. It is therefore *not* possible to use polarization filters to resolve a larger part of the RE momentum space. As illustrated in Figure 2 however, different polarization directions filter out different parts of the synchrotron spot: a vertically aligned polarization filter tends to remove the bright upper and lower edges of the SR spot, while a horizontally aligned polarization filter removes the main body of the SR spot. Therefore, even though the polarized images may look different, they tend to have limited utility in putting further constraints on the RE distribution.

It can be shown that in the limit of vanishing angular spread of the SR (i.e. high RE energy or large detector) no circularly polarized SR is detected. Simulations and experiments however suggest that, due to the finite angular spread of the SR, some circularly polarized radiation can actually be detected. The amount of detected radiation is however very small (typically a few per mille or per cent of the total radiation) since any non-zero contribution must be due to parameter variations (detector/particle distance, magnetic field strength) occuring as the particle's cone of SR sweeps across the detector. Thus, experimental measurements of the circularly polarized SR are sensitive to noise, while numerical simulations require excessively high resolution.

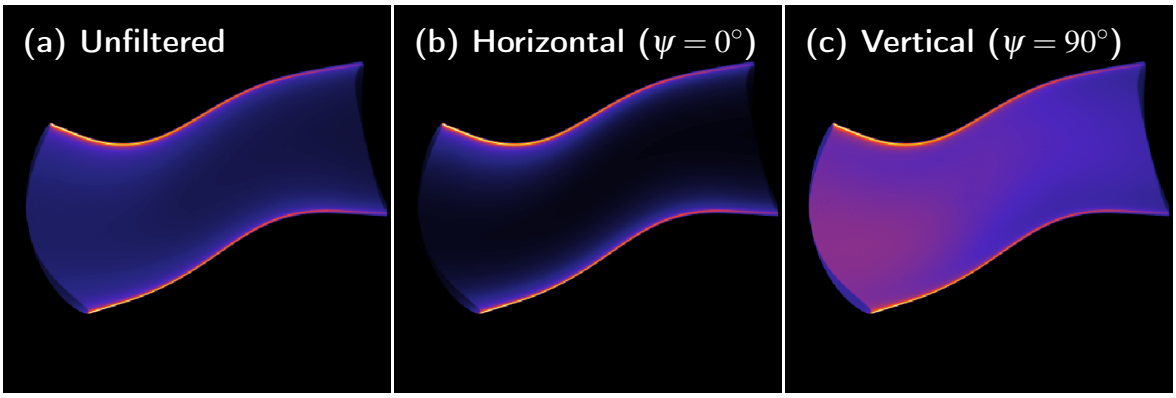


Figure 2: Simulated synchrotron images captured in an ASDEX-U like setup (a) without any polarization filter, (b) with a horizontally aligned linear polarization filter and (c) with a vertically aligned linear polarization filter. The horizontal filter subtracts the body of the spot, whereas the vertical filter partially subtracts the upper and lower edges. All images are normalized to the value of their brightest pixel.

**Accounting for drift orbits** SOFT is based on a zeroth-order guiding-center model, which neglects drifts and assumes that guiding-centers emit a circular cone of radiation centered on magnetic field lines. The high energies sometimes achieved by runaway electrons can however result in significant drift orbits and necessitate a higher order treatment. While the first-order guiding-center equations of motion for relativistic particles are readily available and relatively simple to implement, the *particle* velocity, calculated to the same order, also receives corrections that are more rarely considered in detail [8]. These corrections can become important when studying BR and SR, since both are emitted along the *particle's* velocity vector. In this section we will estimate the relative importance of the guiding-center drifts and gyro-orbit deformations on the measured radiation, and show that in a typical scenario both effects are equally important and that it would therefore be inconsistent to neglect only one of them.

An illustration of how drift orbits and the gyro-orbit deformation affect the detected radiation is shown in Fig. 3(a). While the guiding-center drifts will displace the guiding-center itself by an amount $\Delta X$, the gyro-orbit deformation will lead to the opening angle of the cone of radiation being altered by an amount $\Delta\theta_\mathrm{p}$. Since a particle is only seen by the detector when the cone of radiation intersects the detector, this leads to a displacement of the points from which a particle can possibly emit towards the detector. This perceived displacement in the image is approximately $R\Delta\theta_\mathrm{p}$, where $R$ is the distance between the particle and the detector. To obtain an order-of-magnitude estimate of $R\Delta\theta_\mathrm{p}$ that does not depend on the specific RE and detector details, we take $R \sim R_\mathrm{m}$, where $R_\mathrm{m}$ denotes the tokamak major radius. We can calculate $\Delta\theta_\mathrm{p}$ in first-order theory by numerically maximizing the gyro-averaged angular distribution of

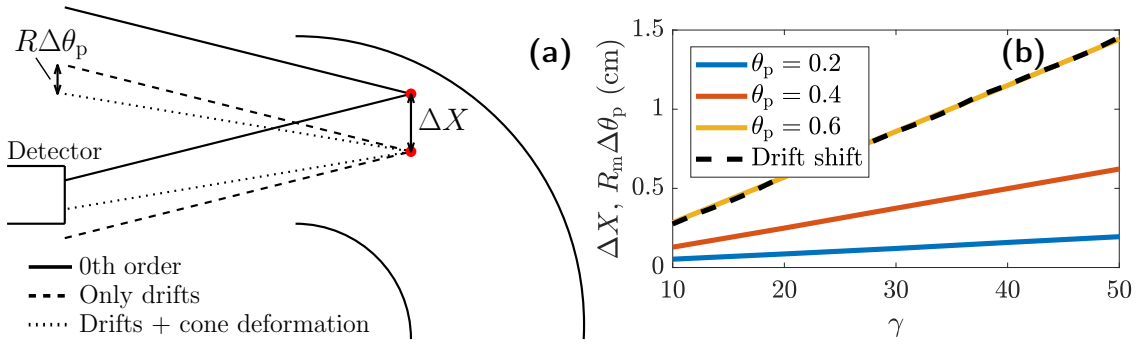


Figure 3: (a) Top view of tokamak. The guiding-center (red dot) emits a hollow cone of radiation with (half) opening angle $\theta_p$ in zeroth order guiding-center theory (solid). The drift orbit shift directly displaces the guiding-center by $\Delta X$ (dashed), while the cone deformation changes the opening angle, resulting in an apparent displacement in the image. (b) Estimated effect of cone deformation $R_m\Delta\theta_p$ (solid) and drift $\Delta X$ (dashed) on an image as functions of particle Lorentz factor $\gamma$ in an ASDEX-U like scenario.

synchrotron radiation

$$\left\langle \frac{dP}{d\Omega} \right\rangle = \left\langle \frac{e^2}{16\pi^2\varepsilon_0 c} \frac{|\hat{n}\times\{(\hat{n}-\vec{\beta})\times\dot{\vec{\beta}}\}|^2}{(1-\hat{n}\cdot\vec{\beta})^5} \right\rangle, \tag{2}$$

with respect to the angle $\mu$ between $\hat{n}$ and $\beta$, so that $\Delta\theta_p = \mu - \theta_p$. Here, $\vec{\beta}$ and $\dot{\vec{\beta}}$ are the normalized speed and accelerations calculated to first order, $\hat{n}$ is a unit vector between the particle and observer and angle brackets denote a gyro average.

Figure 3(b) shows the dependence of the orbit drift shift $\Delta X$ and cone deformation $R_m\Delta\theta_p$ as functions of the particle Lorentz factor $\gamma$ in an ASDEX-U like setup. It shows that the radiation cone deformation is of the same order-of-magnitude as the guiding-center drift shift, both increasing linearly with energy. We can therefore conclude that to consistently simulate the effect of drift orbits on radiation from REs, both the drift and radiation cone deformation must be taken into account. Preferably, such a simulation should also be accompanied by a simulation of the runaway electron distribution function to the same order in guiding-center theory to consistently handle the radius/energy mixing introduced by drift orbits [9], although no such tool is (to our knowledge) yet available.

## References

[1] A. E. Shevelev et al., Nucl. Fusion **58**, 016034 (2017).
[2] A. Tinguely et al., Nucl. Fusion **58**, 076019 (2018).
[3] C. Paz-Soldan et al., Phys. Rev. Lett. **118**, 255002 (2017).
[4] L. Carbajal et al., Phys. Plasmas **59**, 124001 (2017).
[5] M. Hoppe et al., Nucl. Fusion **58**, 082001 (2018).
[6] M. Hoppe et al., Nucl. Fusion **58**, 026032 (2018).
[7] J. M. Stone, *Radiation and optics: an introduction to classical theory*, McGraw-Hill (1963).
[8] A. J. Brizard, Phys. Plasmas **11**, 4429 (2004).
[9] J. Decker, Phys. Plasmas **17**, 112513 (2010).

This work has been carried out within the framework of the EUROfusion Consortium and has received funding from the Euratom research and training programme 2014-2018 under grant agreement No 633053. The views and opinions expressed herein do not necessarily reflect those of the European Commission.